

# Design and Fabrication of the Langley Aerodrome No. 8 Distributed Electric Propulsion VTOL Testbed

David D. North<sup>1</sup> and Ronald C. Busan<sup>2</sup>

*NASA Langley Research Center, Hampton, Virginia, 23681, United States*

Greg Howland<sup>3</sup>

*Analytical Mechanics Associates, Hampton, Virginia, 23666, United States*

The Langley Aerodrome No. 8 (LA-8) is a distributed electric propulsion, vertical takeoff and landing (VTOL) aircraft that is being used for wind tunnel testing and free flight testing at the NASA Langley Research Center. The intent of the LA-8 project is to provide a low-cost, modular test bed for technologies in the area of Advanced Air Mobility which includes electric urban and short regional flight. The methods used on the LA-8 provide a rapid means to verify aerodynamic, acoustic, and flight dynamics analysis of new electric VTOL and short takeoff and landing (STOL) designs. In addition, the flight vehicle will be used to help develop test processes for FAA flight vehicle airworthiness certification and for the development of robust flight control algorithms that are tolerant of failures. A new approach is being used on test vehicle design that makes extensive use of 3-D printing. Although materials used in 3-D printing have less strength than traditional materials used for NASA's wind tunnel and flight models, strategic placement of load-carrying structures allows the aircraft to meet structural criteria while also enabling easy changes to be made in the vehicle design, such as the outer mold line. Modularity of the vehicle's main components allows rapid changes to the vehicle configuration for comparative evaluation of alternate designs. Finally, a description is given of detailed inertia measurements of the flight vehicle using compound pendulum swing methods.

## Nomenclature

AAM-TT	=	Advanced Air Mobility Technology Testbeds
DEP	=	Distributed electric propulsion
ESC	=	Electronic speed controller
Elevon	=	a flight vehicle control device that combines the functions of elevator and aileron
g	=	Earth gravity
GL-10	=	Greased Lightning Electric VTOL
GPS	=	Global Positioning System
LA-8	=	Langley Aerodrome No. 8
MUX	=	Multiplexer switch
NASA	=	National Aeronautics and Space Administration
PCB	=	Printed Circuit Board
RC	=	Radio Controlled
Ruddervator	=	a flight vehicle control device that combines the functions of rudder and elevator
STOL	=	Short Takeoff and Landing
UAM	=	Urban Air Mobility
VTOL	=	Vertical Takeoff and Landing
$\alpha$	=	angle of attack
$\beta$	=	sideslip angle

---

<sup>1</sup> Engineer, Aeronautics Systems Engineering Branch, MS 238

<sup>2</sup> Senior Research Engineer, Flight Dynamics Branch, MS 308, AIAA Member

<sup>3</sup> Engineer, Aeronautics Systems Engineering Branch, MS 238

## I. Introduction

The NASA Advanced Air Mobility Technology Testbeds (AAM-TT) project (formerly called the Rapid Propulsion and Aeronautics Concepts Testbed [RapidPACT] project [1]) was formulated to help meet the technology development needs of the rapidly growing Urban Air Mobility (UAM) effort. Many areas of electric vertical takeoff and landing (eVTOL) research such as distributed electric propulsion, VTOL flight control, aerodynamics of propulsion-airframe interaction, and calibration/validation of aerodynamic and flight dynamics modeling techniques lack a significant underlying database of experimental data. By building and testing wind tunnel models and flight models of a variety of urban air mobility configurations, the AAM-TT project will supply basic data needed for the design and analysis of this new sector of aeronautics. A secondary goal of the project was to develop techniques for improving the fabrication cycle time for small wind tunnel models and free flight models by leveraging new fabrication methods such as additive manufacturing, commonly known as 3-D printing. In addition, use of rapid custom printed circuit board (PCB) services combined with off-the-shelf electronics was used to create a flight control and data recording system capable of measuring approximately 150 aerodynamic and performance parameters and control system inputs and outputs.

The Langley Aerodrome No. 8 tandem tilt wing electric VTOL configuration (Fig. 1) was chosen as the first configuration in a planned series of models, as it is a challenging design which “pushes the envelope” in several areas including distributed electric propulsion (DEP), advanced flight control, and complex aerodynamics. The modular 3-D printed design allows for quick changes to wing cross section, fuselage outer mold line, motor count and motor centerline positions.



**Figure 1. Langley Aerodrome No. 8 (LA-8) electric VTOL in the NASA Langley 12-Foot Low Speed Wind Tunnel.**

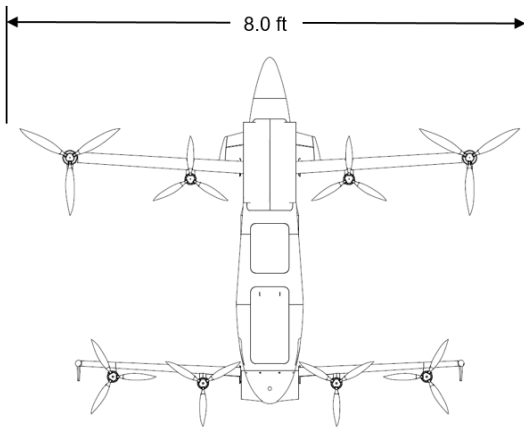


**Figure 2. LA-8 in hover configuration – top view.**

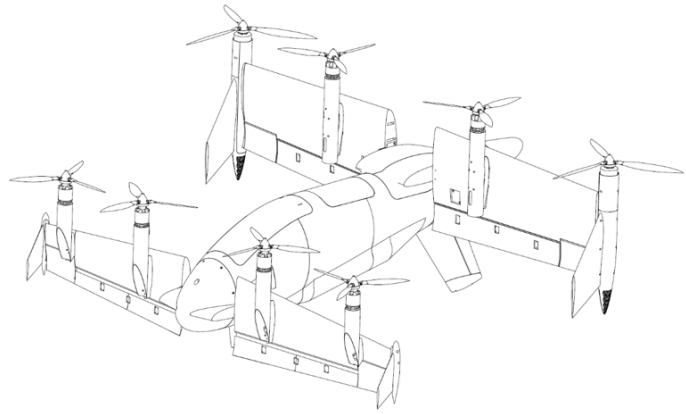


**Figure 3. LA-8 in hover configuration – isometric view.**

The aircraft has two (2) tilt-wings, eight (8) electric motors, four (4) elevons, four (4) single-slotted Fowler flaps, and two (2) ruddervators for a total of twenty (20) independent control actuators (Figs. 2 & 3). Much of the airframe structure is 3-D printed nylon and polycarbonate with some use of carbon fiber and aluminum for spars and internal fuselage walls.

## II. Concept Ideation

There was a desire to start the planned series of testbeds with a challenging design that would capture many of the features seen in complex Urban Air Mobility concepts being proposed by industry. Several concept configurations from previous NASA electric VTOL projects (Fig. 4) and new ideas (Fig. 5) were compared in a selection process that included criteria such as aerodynamic performance, flight control complexity (high complexity was considered good), and relevance to industry concepts. In addition, there was specific research interest in high lift devices combined with distributed electric propulsion (i.e. “blown” wings and flaps). The tandem tilt-wing configuration scored the best when considering all criteria.

After the selection of the overall tandem tilt-wing layout, several aerodynamic design iterations were performed using first principles analysis and several analysis tools such as OpenVSP and XFLR5 to arrive at a design that met acceptable performance and stability characteristics [2].

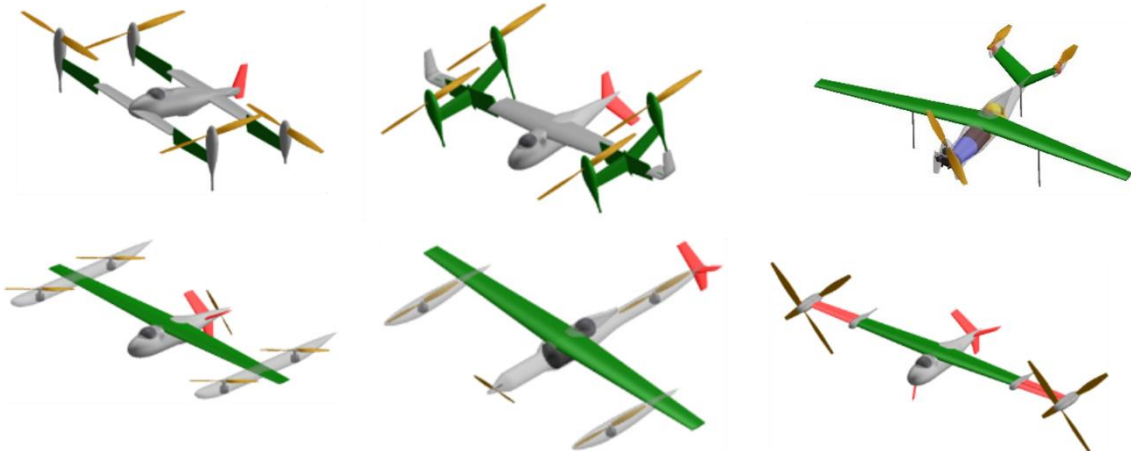


**Figure 4. NASA eVTOL Concepts considered for the Advanced Air Mobility Technology Testbed Project.**



**Figure 5. Early eVTOL concept configuration developed for the Advanced Air Mobility Technology Testbed Project.**

### **III. Airframe Mechanical Design and Fabrication**

The LA-8 was designed such that the same airframe could be used as both a wind tunnel model and a free flight model. While a common wind tunnel model / flight model approach can potentially cause non-optimal characteristics (e.g. wind tunnel model strength could be too low and flight model weight could be too high), a single model has resulted in significantly less design and manufacturing effort spent compared to two separate models, while meeting strength and weight requirements. The model required attachment points and access panels for mounting to the wind tunnel sting and balance (Fig.6). The tip-to-tip rotor distance of the model, 8.0 feet, was sized to fit within the limits of the NASA 12-Foot Low Speed Tunnel. Initially, a combined 3-D printing with composite over-wrap was considered for the outer skin of the aircraft [1]. After further stress analysis and subcomponent strength testing, it was decided to not use a composite over-wrap to save fabrication time. Commercial off-the-shelf (COTS) components such as motors, propellers, and servos were used to the extent possible.

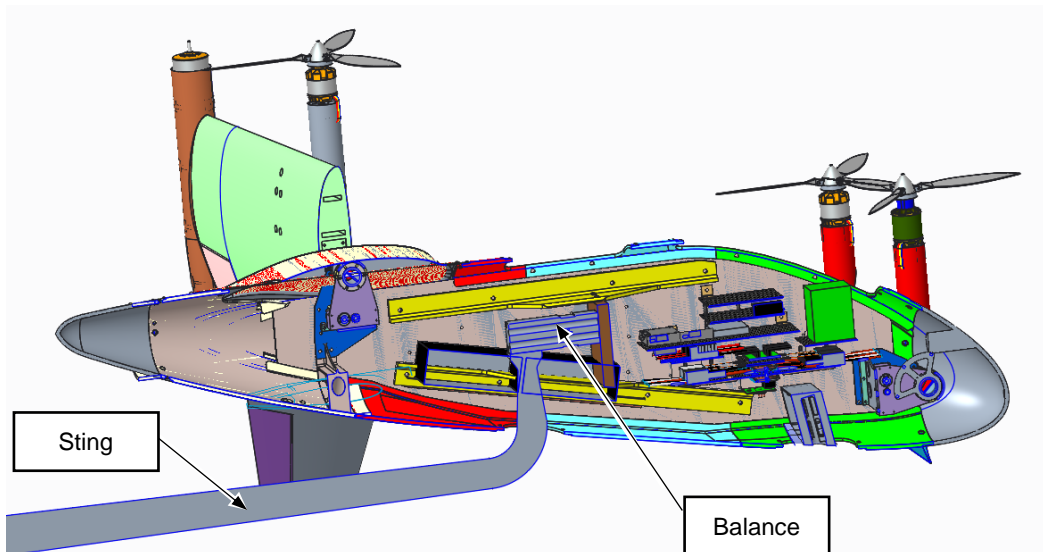


**Figure 6. Cross section of LA-8 showing mounting arrangement on the wind tunnel balance and sting.**



A decision was made early in the program to incorporate as much 3-D printing as feasible into the design of the LA-8. The primary goal was to compare design and fabrication benefits of 3-D printing with previously used fabrication techniques such as molded composites. A secondary goal was to develop new design and fabrication techniques for future models using 3-D printing.

3-D printers used on the LA-8 airframes included the following printer models and materials:

- Stratasys 360 – Materials: nylon, polycarbonate
- Markforged Mark II – Material: Onyx, nylon with infused carbon fiber. Secondary layers of continuous carbon fiber were added in layers of some parts to increase strength.

To reduce weight and maintain aircraft outer mold line surface profile tolerance, most of the larger parts were designed with honeycomb sandwich walls. The thickness of the honeycomb sandwich infill varied with the sizes of the parts. Most parts are approximately 0.25 inch thick honeycomb with honeycomb cell size ranging from 0.188 inch to 0.125 inch. The carbon infused nylon parts (Onyx material) used triangular fill, when applicable. The outer surface faces of the honeycomb sandwich are 0.014 inch thick.

Both wings and fuselage are divided into multiple smaller parts to avoid the risk of print malfunctions and the associated excessive print time for large parts. The process of manufacturing multiple smaller parts was adapted from a lesson learned on previous projects where print failures drove project schedule. Parts are bonded together after printing and included alignment features or holes for pins to aid in alignment during assembly. Many of the parts printed were used “as printed” with no additional work. Other parts required removal of internal soluble support structure, tapping, installation of threaded inserts, drilling of holes for dowel pins, and surface preparation for painting.

## A. Wing Design and Fabrication

The aft main wings are fabricated in three (3) 3-D printed sections and bonded together (Fig. 7). 3-D printed motor nacelles with internal carbon tubes for motor support are bolted to the wingtip of the aft wings. The outboard nacelles also contain servos that drive the elevons directly. The elevon servo horns are fastened to a drive adapter that directly engage the outboard end of the elevon and also serve as the outboard elevon hinge. The three wing sections are bonded together with a single cylindrical carbon spar that spans across the three sections. The carbon spar is bonded into a short aluminum spar at the root of each wing. The short aluminum spar is plugged into the wing tilt mechanism in the fuselage. The flaps are built in two sections and printed using polycarbonate material. Length-wise

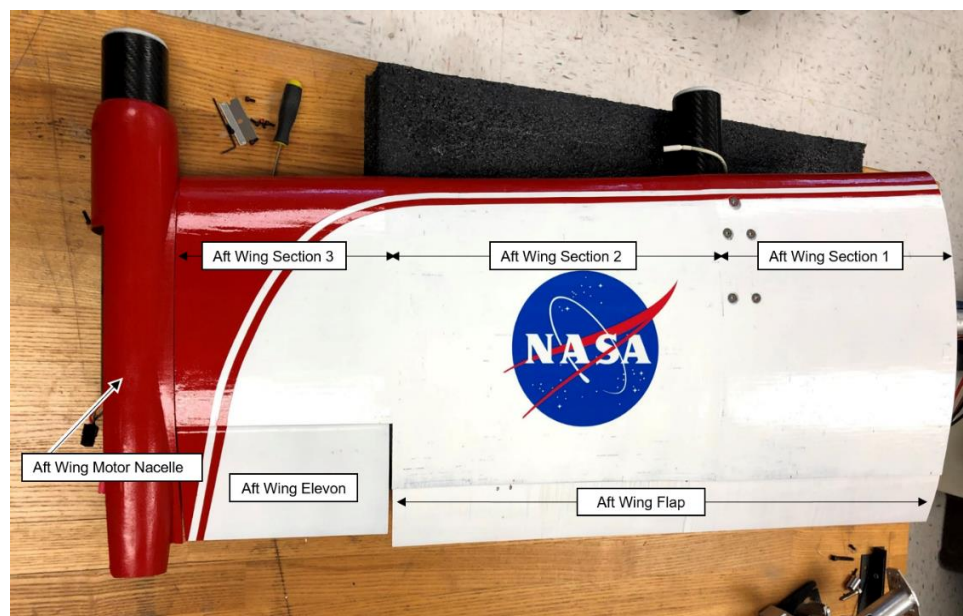
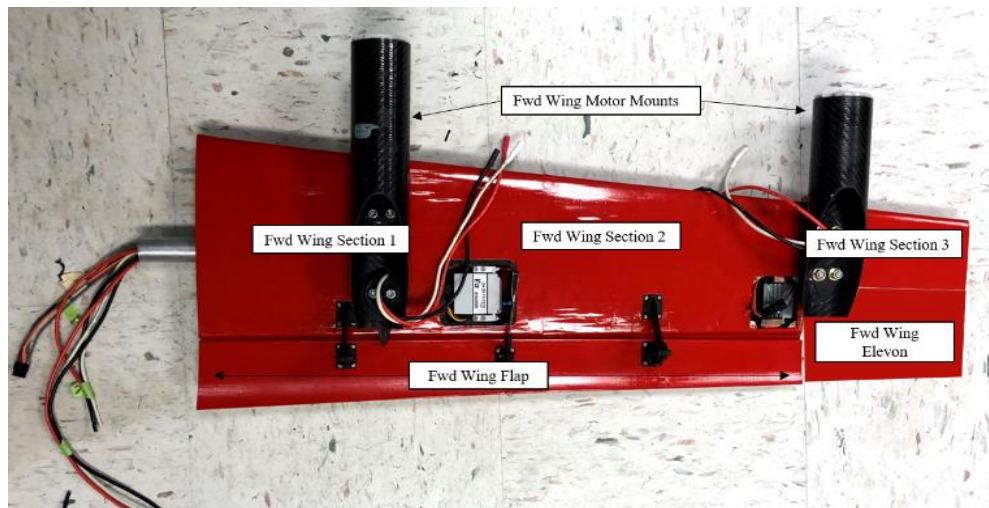


Figure 7. Aft left wing – Top Side.

holes are designed into the flaps to accept carbon fiber tubes for alignment and reinforcement. The full-length alignment tubes are bonded into the flap halves. The flap hinges are 3-D printed using Onyx material. Additional continuous carbon fiber was added by the printer during the print process to selected layers of the hinges to increase strength and stiffness.

The forward wing sections were 3-D printed and assembled onto a metal and carbon fiber spar similar to the aft wing (Fig. 8). The motor mounts consist of 2 inch carbon tubes with 3-D printed inserts at the forward end for motor attachment and inserts in the aft end to spread out loads for the attachment screws, which pass through 3-D printed pylons before entering hard points in the wing.



**Figure 8. Forward left wing – bottom side.**

## B. Fuselage Design and Fabrication

The main fuselage construction consists of six (6) 3-D printed sections. The four (4) middle sections (Fig. 9) are connected by a pair of commercially available 0.25” thick carbon foam core sandwich panels spaced six (6) inches apart that create the backbone of the fuselage (Fig. 10). The initial plan was to wrap the exterior of the 3-D printed fuselage in carbon fiber for added stiffness. However, it was later determined that the structure was very stiff and the additional external wrap was not needed.

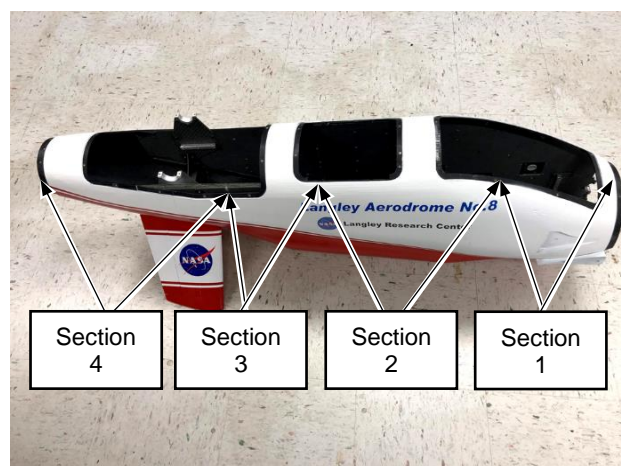


**Figure 9. LA-8 fuselage.**

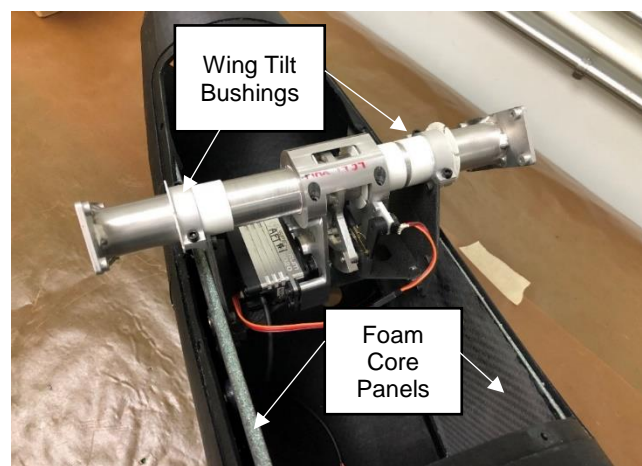


**Figure 10. Aft fuselage section structural carbon fiber foam core sandwich panels and wing tilt drive mechanism.**

NACA ducts were incorporated into the sides of the forward fuselage (Fig. 11) to allow airflow into the fuselage for cooling of the electrical and avionics systems. The tail cone (Fig. 12) has an open honeycomb structure to allow airflow out of the fuselage.



**Figure 11. LA-8 removable nose section and NACA inlet ducts.**



**Figure 12. LA-8 tailcone showing honeycomb air outlet.**

The nose (Fig. 11) and tail sections (Fig. 12) were designed to be removable for access to the fore and aft internal areas of the fuselage. The nose section has reinforcing ribs and mounting provisions for an aerodynamic probe that can measure airspeed, angle of attack ( $\alpha$ ) and sideslip ( $\beta$ ). Five access (5) hatches, two (2) lower and three (3) upper, were incorporated into the fuselage design. The two lower hatches are for the forward landing gear bulkhead access and for wind tunnel sting and balance mounting. The three (3) upper hatches are for access to electronics systems, battery installation and removal and aft wing removal. Nylon plugs with threaded inserts are incorporated into the carbon side panels for attachment of wind tunnel mount hardware, electronics boards mounting brackets and battery support brackets.

### **C. Inverted V-Tail Design and Fabrication**

At landing, the aircraft rests on a small airfoil-shaped skid on the lower forward area of the fuselage and the tips of the two inverted V-tail stabilizers at the aft end of the aircraft. The V-tail surfaces are attached to the fuselage and supported their full length with carbon tubes secured to a bulkhead in the aft section of the lower fuselage (Fig. 13). The aft bulkhead also contains mounts for servos that drive the ruddervators via torque tubes. The lower section of the ruddervators use a 0.25 inch carbon tube as a pivot pin. A wheeled landing gear system has been designed for future short takeoff and landing (STOL) testing, but is not included in the first instantiation of the LA-8.

### **D. Finish Work and Painting**

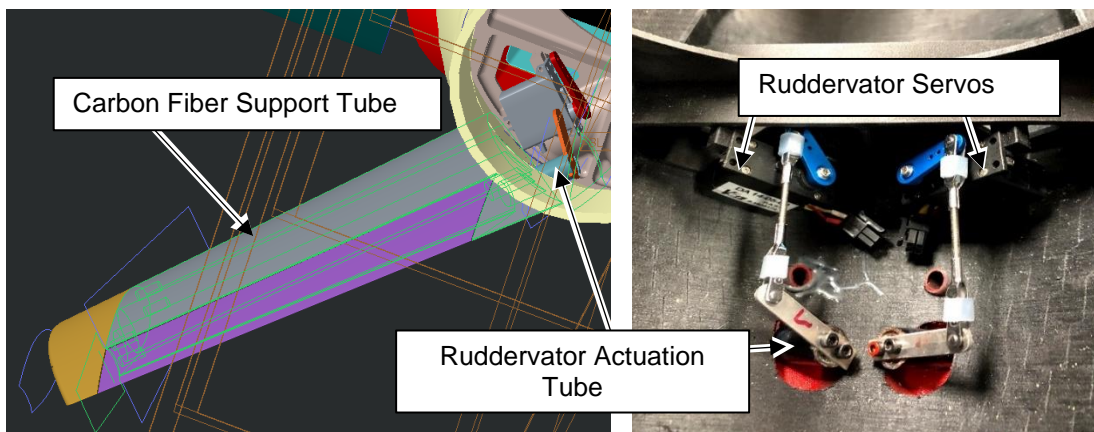


**Figure 13. V-Tail mounting and ruddervator drive mechanism.**



The outer surface of the first LA-8 airframe (blue/white) was prepared and painted to create a smooth and uniform finish. Surface bond lines and imperfections in the 3-D printed parts were filled with glazing putty and sanded. Several layers of automotive primer paint were applied with sanding after each layer. Three layers of acrylic urethane paint were applied for a final finish.

In order to save weight and time, much less effort was put into the painting of the second airframe (red/white). Minor imperfections in the printed parts were left as-is, and putty was only used for areas that stood out or would severely affect aerodynamics. After sanding, a light coat of automotive 2K primer was applied followed by just enough acrylic urethane top coat to achieve a uniform color. For this airframe, all parts were weighed before and after painting. Total paint weight for the entire airframe was 0.6 pounds.

## E. Wing Tilt Mechanism Design and Fabrication

One of the goals of the AAM-TT project is to improve the design, build, and test process that had been used in the development of previous wind tunnel and flight models. The most recent and relevant aircraft for comparison is the GL-10 electric VTOL [3]. The GL-10 wing actuation system used an industrial linear actuator. While it had excessive strength, it was heavy and slow. The actuator required a large mounting bracket and a substantial crank arm on the wing pivot to drive the rotation. Additional compression tubes were used to tie the actuator mount bracket structure to the wing pivot structure to react to the actuator loads.

The development of the wing tilt mechanism for the LA-8 airframe (Fig. 14) was focused on reducing the weight and increasing the speed of wing tilting actuation. A relatively inexpensive off-the-shelf RC servo was used to drive a reduction gear set to achieve the required output torque and wing tilt speed. Standard RC servos only have a nominal 90 degree rotation range, therefore the servo was modified to run continuously by removing the internal potentiometer and also removing the rotation limiting tang on the servo internal output gear. The position feedback potentiometer removed from the servo was mounted remotely while still providing signal to the servo with an extension cable soldered to the servo control board. A crank arm and linkage system connected to the potentiometer to the main wing tilt torque tube.

The aluminum torque tubes in the wing tilt mechanisms also serve as the wing load carry-through. The outer diameter of the torque tube is 1.25 inches and the inner diameter is 1.00 inches. The wing spars plug directly into the inner diameter of the torque tube. The wing tilt torque tube was designed to carry the wing load during worst case scenarios in flight. The torque tube also acts as a conduit for all wiring from the wings into the fuselage. Sleeve bushings were mounted to the fuselage structure to support the shaft and transfer loads to the fuselage. An insert was 3-D printed and installed inside of the torque tube to guide wires during installation of the wing.

The LA-8 wing tilt mechanism and associated hardware realized a 2.6 pound weight savings or 65% less per mechanism relative to the GL-10 wing tilt mechanism. In addition, the compact size of the mechanism frees up valuable space in the fuselage for other research components.

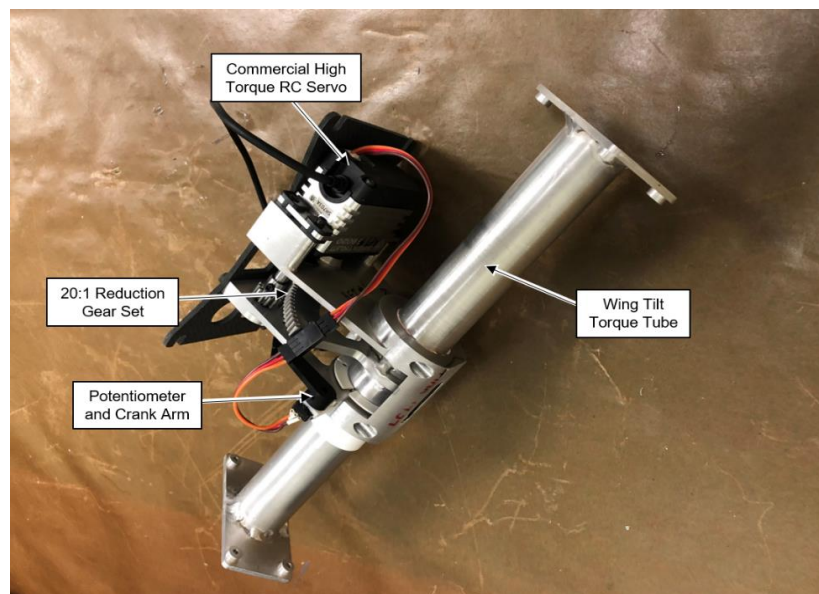


**Figure 14. Wing drive mechanism used on forward and aft**



## IV. Structural Analysis and Testing

A comprehensive stress analysis of the LA-8 airframe was performed during the design process using NASA standard 1710.15 *Wind Tunnel Model Systems Criteria*. Load cases for analysis included worst case loading expected in both wind tunnel and flight conditions. Several load tests on a structural test article and the actual model were conducted to verify that the airframe design met the structural criteria.

Prior to fabrication of the actual airframe wings, a simplified concept wing section was fabricated for subcomponent structural testing. The structural criteria for the wings included a three (3) *g* load in normal flight, and a two (2) *g* load in inverted flight. The tested wing section was loaded incrementally until failure. Based on an all up weight of 65 pounds, the wing spar at the root of the wing yielded at a 6.4 *g* loading and failed at an 8.9 *g* loading. This was well beyond the expected flight loads and gave the design team confidence to proceed with the hardware and techniques used in the sample wing section.

Prior to wind tunnel testing, additional load tests were performed on the completed airframe. Test fixtures were designed and fabricated to support the airframe to tunnel mount hardware in the fuselage similar to the manner that it would mounted in the wind tunnel (Fig. 15). Distributed loads were applied with lead shot bags to all four (4) wing segments to represent three (3) *g* normal loading and two (2) *g* inverted loading. Additionally, the wind tunnel testing itself became a form of structural testing as many of the components were tested beyond their operational envelope for normal flight conditions. The wind tunnel testing identified an issue with elevon servo torque and over-current that resulted in failure of several servos. The elevon design was modified with larger torque servos.



Figure 15. Structural load testing fixture.

## V. Power System, Flight Control and Data Recording Design and Fabrication

### A. Power System

In order to facilitate a rapid design and fabrication process, the LA-8 power system is designed with a combination of COTS parts and custom, rapidly prototyped printed circuit boards PCB (Fig.18). The electrical power to the entire aircraft is supplied by two commercially available lithium polymer 8-cell (33.6 volts maximum) 22000 mAh batteries. The battery voltage is supplied to eight (8) Castle Creations Phoenix Edge Lite 100 amp ESCs which supply three-phase power to eight (8) Scorpion SII-4035 kV 450 electric motors. Three (3) Aeronaut CAM Carbon folding 16 inch x 8 inch pitch blades are used on each of the four (4) motors. Custom injection molded blades that are a mirror of geometry of the COTS blades were manufactured to enable opposite rotation of propellers by the other four (4) motors. Custom blades with opposite rotation direction are critical in order to have a net neutral torque load imparted on the vehicle from motor / propeller torques.

Four Castle Creations BEC Pro 20 amp switching voltage regulators are used to supply regulated voltage ranging from 5.5 volts to 12.0 volts to servos, fans, and avionics. An additional custom PCB DC-to-DC converter was designed and fabricated to supply ground isolated power to the  $\alpha$ - $\beta$  aero probe transducer and Raspberry Pi in the data recording system. Care was taken in the design of the power system to ensure that “ground loops” caused by differentials in ground voltage in different parts of the power system do not cause deleterious effects.

A redesign of the power system was needed after thermal testing showed ESC temperatures exceeding manufacturer's recommended temperature limits. Additional cooling fans and a 3-D printed duct system that directs cooling air over the ESCs were mounted in the foam core fuselage sidewalls to lower the ESC temperature (Fig. 16 & 17). Heat sinks with cooling fins were also bonded to the surface of the ESCs to aid in cooling.

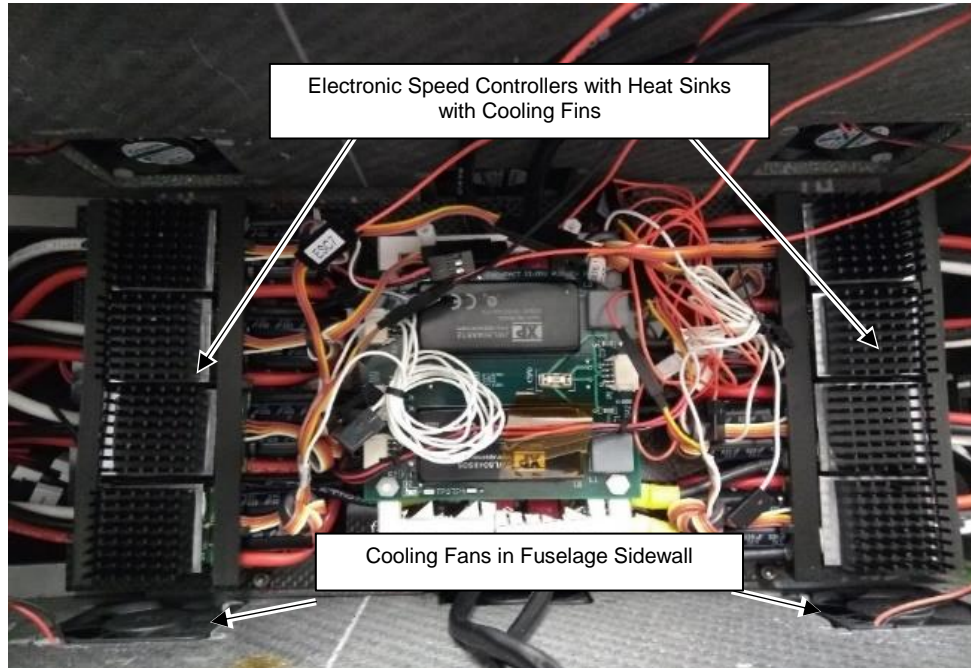


**Figure 16. Electronic speed controller arrangement showing sidewall cooling fans (cooling duct removed to show ESCs with heat sinks and cooling fins).**



**Figure 17. 3-D printed cooling duct for ESC cooling.**

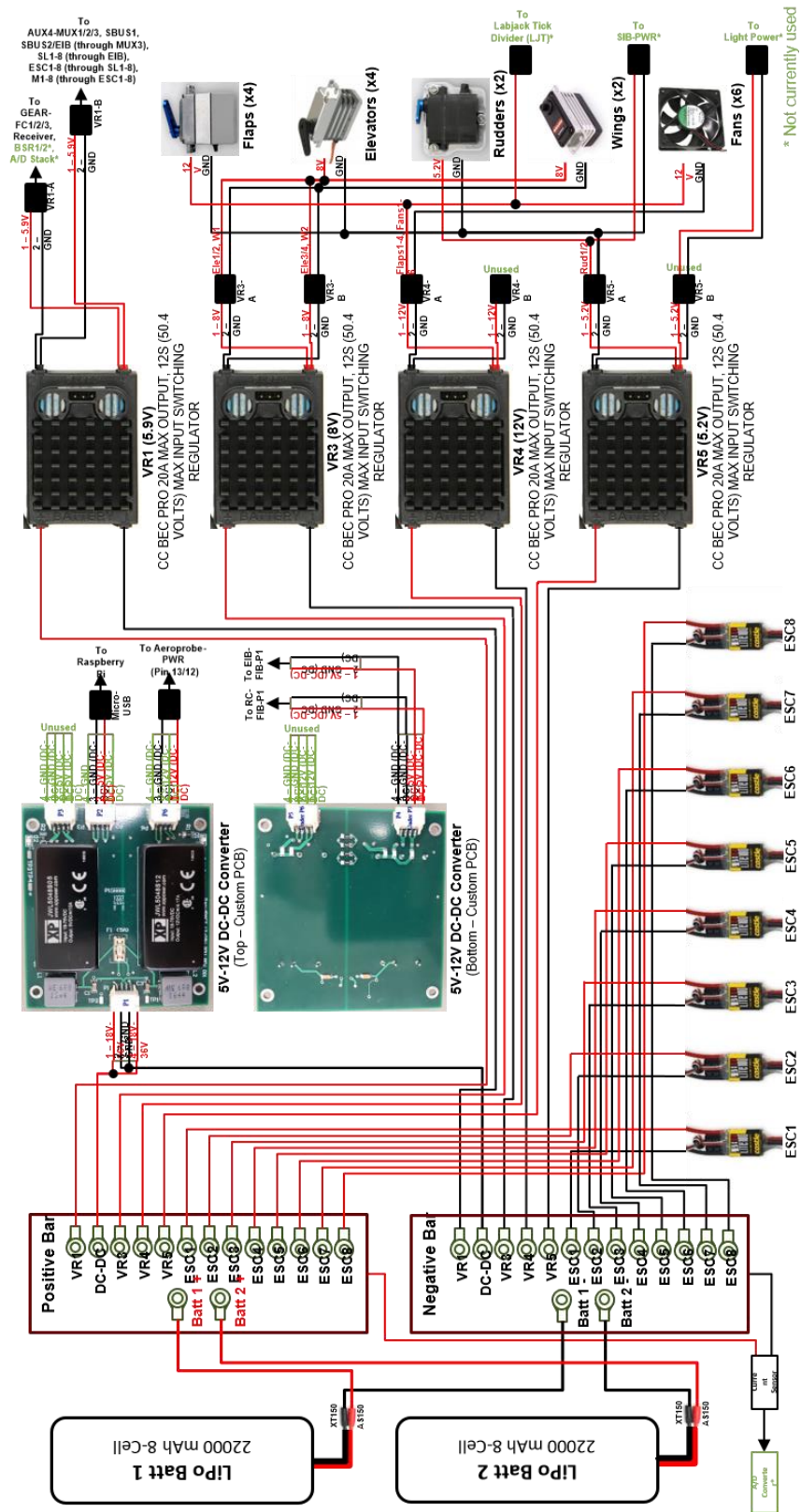


Figure 18. L.A-8 Power System.



## B. Flight Control System

The LA-8 flight control system is based on the successful flight control system used on the GL-10 aircraft (Fig. 19). Three (3) KK2.1.5 boards are used in parallel to provide the twenty (20) flight control outputs required. Figure 19 shows the allocation of control outputs to ESCs and servos. The KK2.1.5 boards run the open-source firmware OpenAeroVTOL for hover, transition, and forward flight control. The KK2.1.5 board with OpenAeroVTOL is not a full autopilot. The flight controller provides the specialized stabilization and mixing functions for VTOL control, but does not have the capability for GPS waypoint navigation.

A COTS transmitter and receiver is used to receive pilot signals. The pilot has control of motor speed, pitch, roll and yaw axes of the aircraft in hover mode, forward flight mode, and transition mode (i.e. between hover and forward flight). A fifth input channel, a three (3) position toggle, on the transmitter is used to send the flight mode signal.

To accommodate future research with alternate flight controllers, autopilots and flight control algorithms, three multiplexer switches are placed downstream of the KK2.1.5 to allow flight control signals to be switched from the KK2.1.5 boards to the research flight controller via a radio signal from the transmitter.

A custom PCB was designed to transfer power and signals to eight Castle Serial Links. The Serial Links allow the data recording system to gather data from the ESCs and also allow real time telemetry of ESC data.

## C. Data Recording System and Telemetry

Like the power system, the LA-8 data recording system is designed with a combination of COTS parts and custom, rapidly prototyped PCBs (Fig. 20). Due to the unknown nature of future testing with the aircraft an extremely capable data recording system was desired to encompass a large variety of flight testing data types. The data recording system can record 148 separate parameters including airspeed, angle of attack ( $\alpha$ ), sideslip angle ( $\beta$ ), servo positions, motors speeds, motor power, battery voltage, vehicle state data (relative angles to gravity vector, linear and angular rates and accelerations), command signals, and flight controller signals.

Custom data recording software was written to record data on a Raspberry Pi 3 Model B+ single board computer. Data from most sensors is processed through signal converters and gathered into a CAN bus system that delivers time-stamped data to the Raspberry Pi. The Vector Nav 200 inertial measurement unit (IMU) delivers serial data directly to the Raspberry Pi. The Aeroprobe airspeed and  $\alpha$ - $\beta$  probe delivers data to a real-time clock that time stamps data and then sends the data to the Raspberry Pi. Custom PCB carrier boards were designed to hold two Adafruit Feather board microprocessors which are used to convert pulse width modulation signals and other serial data from sensors into CAN bus format.

The LA-8 uses the commercially available telemetry software system COSMOS to send low-rate data of select parameters to a ground station via a 900 MHz radio system.

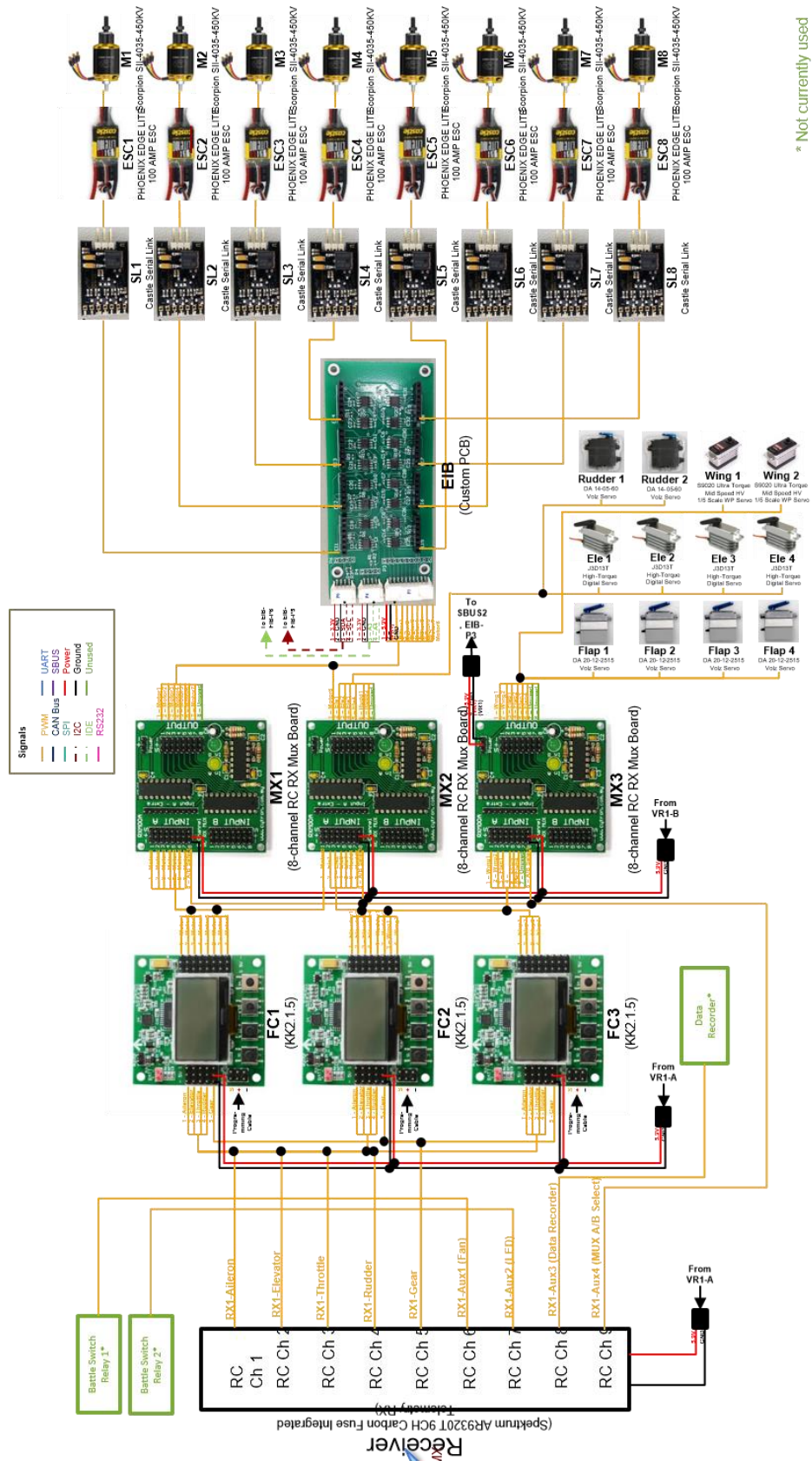


Figure 19. Flight Control System.

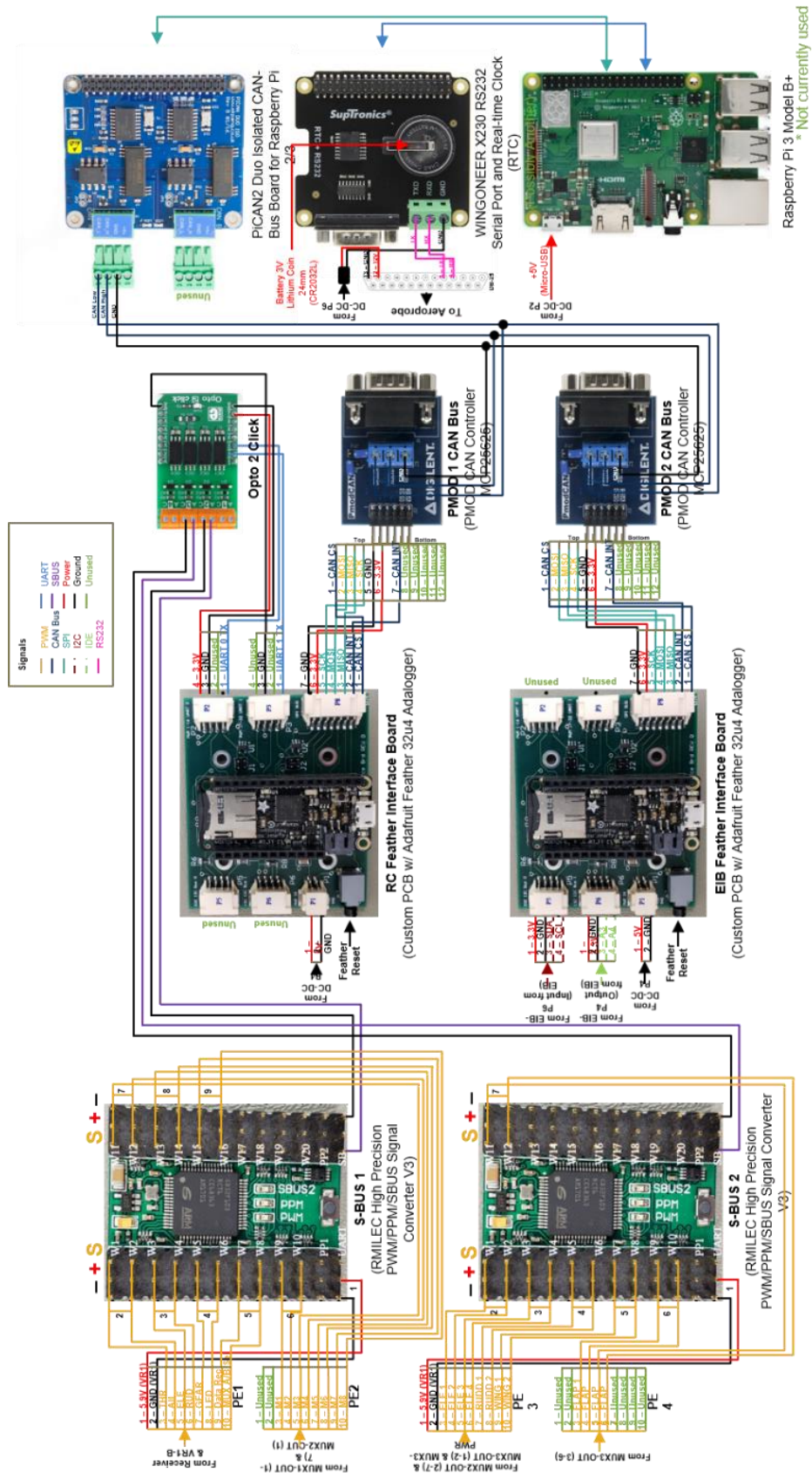


Figure 20. Data Recording System.



## VI. Mass Properties Testing

### A. Test Setup/Apparatus

Yaw inertia and off-axis measurements to get the cross-product  $I_{xz}$  value and the angle of the principal axis were done with a quad-filar torsional pendulum. The quad-filar torsional pendulum had upper and lower aluminum rings nominally 32 inches in diameter connected by lengths of cable. One set of inertia measurements was taken using 12 feet long cables, and a second set of measurements was taken with 9 feet long cables. To eliminate set-up time associated with determining the center-of-gravity (CG) fore-aft position for different wing angles and placing this at the center of rotation, an arrangement was used which allowed the airframe to self-align the overall CG below the center of the lower aluminum ring. Two (2) braided fishing line cords attached to anchors points in the fuselage went up around pivot points on either side of the lower aluminum ring. These cords are highlighted in green and red in Figure 21.

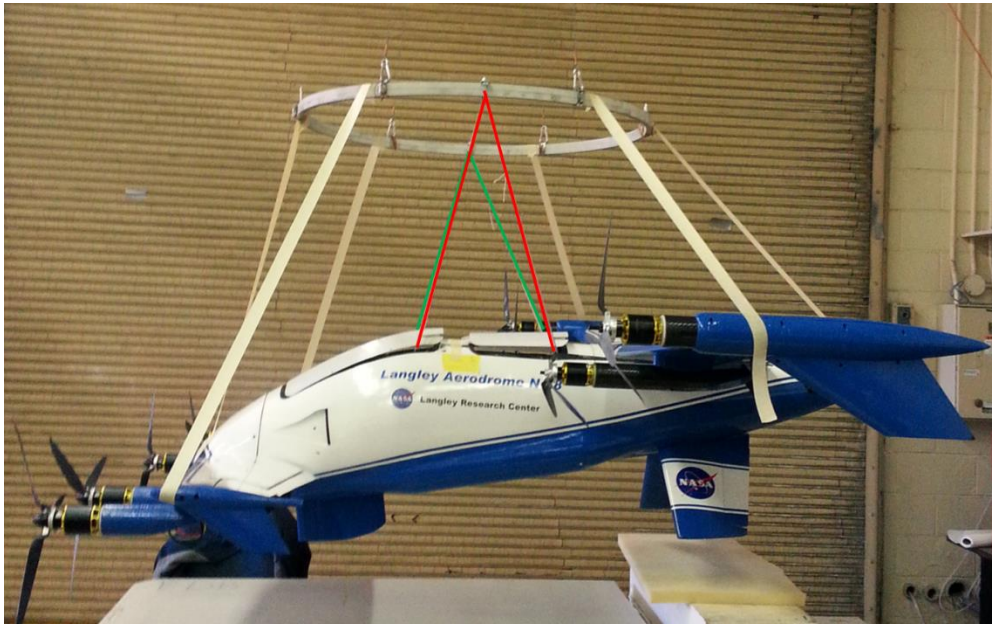


**Figure 21. LA-8 on Quad-Filar Torsional Pendulum – Self-Aligning CG Features Highlighted**

The amount of each cord behind and in front of the pivots was adjusted until the airframe hung level. A plumb bob which hung down from the center of the aluminum ring was used to locate the position of the CG on the top of the fuselage relative to a reference mark. This set-up showed a 1.1 inch shift aft for the overall CG when the wings were rotated from  $0^\circ$  to  $90^\circ$  - which matched the shift measured previously in bench testing. Before any inertia measurements were taken, pieces of masking tape were added to prevent any relative motion between the lower aluminum ring and the airframe when a torsional oscillation was induced.

Pitch and roll inertias were determined using a method where the airframe is rotated about an overhead pivot. Figure 22 is from a 1986 weight engineer's handbook – showing the equation and critical parameters. Since the location of the airframe CG in the vertical direction was not known, multiple measurements were taken with the pivot being at different distances above the top of the fuselage outer mold line (OML) and then the distance of the CG below the top of the fuselage OML was determined using a graphical method where the CG position was treated as a variable. The plot in Figure 22 shows the results for three different pivot distances. It was determined that the actual vertical position of the CG must be approximately 6.75 inches below the fuselage top OML for the wings at  $0^\circ$ .

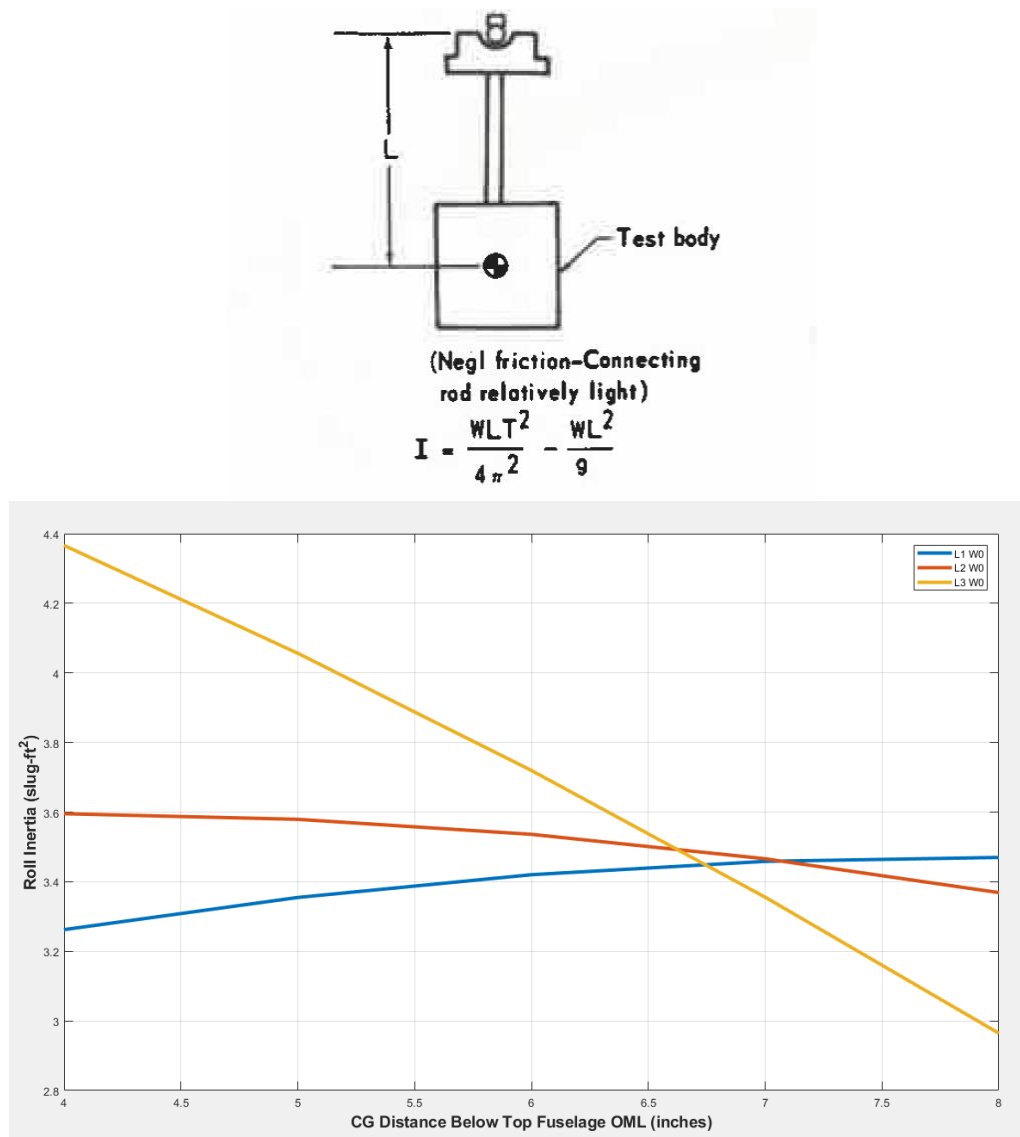


**Figure 22. Swinging Pendulum Equation, and Graphical Method for Determining Vertical CG Location.**

The magnitude of the vertical CG shift in the overall CG should match the horizontal shift - and this delta was assumed. (Less data was taken for the wings at 90°, so engineering judgment was used – rather than taking additional data). Using the CG locations previously determined, the range of calculated inertias for most of the individual measurement trials used fell within  $\pm 1.5\%$  - with only one or two being closer to  $\pm 2\%$ .

After all measurements were taken, it was determined that the hatch opening on the top of the fuselage that was assumed level was actually at  $\sim 1.3^\circ$  nose up. This was corrected with regard to the fore-aft CG location, but after observing a negligible effect on other parameters, it was decided not to make corrections to any of the inertias.

A 0.25 inch lateral CG deviation off the centerline was measured, but no attempt was made to correct it. This deviation has a minor impact on the inertias and can be corrected later, if deemed necessary.

Air damping corrections are also not included in this mass property assessment. Previous mass property assessments for another single-wing airframe of similar overall size and weight produced pitch and roll air damping estimates of 1.5% and 2% respectively. Rough calculations based on a comparison of the mass distribution and surface areas of this airframe and the LA-8 indicated that air damping for the LA-8 would likely be closer to 1% - so a detailed assessment based on additional measurements was not done.

## B. Summary of LA-8 Mass Property Assessment Results

- Assembled Weight = 62.65 lbs
- CG Location with Wings at 0°: X = 23.75 inches, Z = 6.23 inches, & ~0.25 inches left of centerline
  - Note: Datum for CG measurements is the most forward point of the aircraft nose
- CG Location with Wings at 90°: X = 24.85 inches, Z = 7.33 inches, & ~0.25 inches left of centerline
- $I_{roll\_Wings\_0^\circ} = 3.462 \text{ slug-ft}^2$
- $I_{roll\_Wings\_90^\circ} = 3.581 \text{ slug-ft}^2$
- $I_{pitch\_Wings\_0^\circ} = 3.446 \text{ slug-ft}^2$
- $I_{pitch\_Wings\_90^\circ} = 3.531 \text{ slug-ft}^2$
- $I_{yaw\_Wings\_0^\circ} = 6.497 \text{ slug-ft}^2$
- $I_{yaw\_Wings\_90^\circ} = 6.471 \text{ slug-ft}^2$
- $I_{xz} = 0.867 \text{ slug-ft}^2$ , Principal axis in XZ plane angled nose-down 14.9°

Based on the differences between the various measurements taken, the mass moments of inertia listed above are estimated to be accurate within  $\pm 3\%$ , and CG locations with 0.05 inches.

The results indicate very little difference in the mass moments of inertia about the CG resulting from changing both wing angles between 0° and 90° - although there was fore-aft and vertical overall CG location shift. Further analysis indicated that this was a predictable consequence of the LA-8's particular geometry, mass distribution, and having the wing angles matching at all times – and is not a result that one should assume for other tandem tilt wings. Since the LA-8 mass moment of inertia changes associated with wing tilt angle fall within the estimated accuracy of those measurements, it is suggested that using constant  $I_x$ ,  $I_y$ , and  $I_z$  inertias and only correcting for the CG shift associated with wing tilt is a reasonable simplification that should still give good results for LA-8 simulation and control design efforts.

## VII. Lessons Learned

Some of the significant lessons learned in this first research test aircraft of the AAM-TT project which will be applied to the new aircraft planned in the series are listed below:

- 1) Creating an aircraft that can be used for both wind tunnel testing and flight testing is viable and can save significant time and money versus two models. Design requirements for the wind tunnel testing and flight testing, such as weight and structural criteria, must be considered early in the design process.
- 2) 3-D printing is a viable method for reducing the manual labor required for a small-scale research wind tunnel model and flight model but will probably result in a higher weight.
- 3) Slight differences in custom propeller blade profiles can make a big difference (up to 15%) in thrust performance.
- 4) Custom flight control avionics and data recording will most likely be the highest hour task in the development of a new small research aircraft
- 5) ESCs need significant cooling and should include air cooling features. Placing the ESCs flush with the OML to allow cooling airflow should be the first choice.
- 6) Custom printed circuit boards can reduce a large amount of power and signal wiring. They are easily designed with commercial software and can be rapidly manufactured in days.
- 7) Actual servo torque and speed should be verified with bench testing
- 8) Nylon 3-D printed parts can deform significantly in the hot liquid bath used to dissolve the support material if the bath temperature is not closely controlled.
- 9) Part size of 3-D printed parts should be kept smaller to avoid a large investment of time that may be lost if the print fails late in the print process.



## VIII. Conclusion

The LA-8 electric VTOL technology testbed has proven to be a significant asset for providing data to the UAM effort. The exploration of alternative design and fabrication methods that leverage new rapid prototyping techniques such as 3-D printing and rapid printed circuit board design and fabrication has provided useful information on the pros and cons of the new techniques. 3-D printing enables the fabrication of complex parts without the need for expensive and time consuming machining and molding of composite parts. While current 3-D printing materials have low strength that will likely result in an airframe weight that is higher than a composite molded structure, strategic placement of composite structural components within a mostly 3-D printed airframe can be designed to meet strength requirements. Careful inertia measurements are critical for free flight dynamics testing and were performed on the LA-8 with a torsional pendulum apparatus.

## Acknowledgements

The Advanced Air Mobility Technology Testbeds project would like to acknowledge the funding and support provided by the following groups to design and fabricate the LA-8:

NASA Transformative Aeronautics Concepts – Convergent Aeronautics Solutions  
NASA Transformative Aeronautics Concepts – Transformational Tools and Technologies  
NASA Flight Demonstrations and Capabilities

Thanks to the following contributors to the project:

Greg Howland	Lead, mechanical design engineer and lead fabrication
Steve Geuther	Aerodynamic design, analysis and wind tunnel test
Robert McSwain	Project Manager, system design and system test
Neil Coffey	Lead, Data acquisition system design, software design and test
David Hare	Power system design, data acquisition system design, fabrication and test
David Bradley	Test pilot and fabrication
Mark Cagle	Mechanical design
Jared Fell	Mechanical design
Lou Glaab	Test pilot
Brian Duvall	Power system design and fabrication and wind tunnel test
Toby Comeaux	Power system and data acquisition system fabrication
Justin Lisee	Power system and data acquisition system fabrication
Mike Langford	Structural analysis and test
Chris Meek	Fabrication and flight test
Mark Frye	Flight test
Dan Healey	Flight test
Scott Sims	Flight test
Pat Murphy	Wind tunnel test
Ron Busan	Wind tunnel test, mass properties test
Ben Simmons	Wind tunnel test, aero modeling
David Hatke	Wind tunnel test
Earl Harris	Wind tunnel test
Rose Weinstein	Wind tunnel test
Lee Pollard	Wind tunnel test, photography
Sue Grafton	Wind tunnel test
Sam James	Fabrication
Gary Wainwright	Fabrication
Rob Andrews	Fabrication
Kevin Krohto	Fabrication
Don Smith	Fabrication

## References

<sup>1</sup>McSwain, R.; Geuther, S.; Patterson, M.; Whiteside, S.; North, D.; Howland, G.: *An Experimental Approach to a Rapid Propulsion and Aeronautics Concepts Testbed*. NASA/TM– 2020-220437.

<sup>2</sup>Geuther, S.; North, D.; Busan, R.: *Investigation of a Tandem Tilt-Wing VTOL Aircraft in the NASA Langley 12-Foot Low Speed Tunnel*. NASA/TM-20205003178.

<sup>3</sup>McSwain, R.; Glaab, L.; Theodore, C.; Rhew, R.; North, D.: *Greased Lightning (GL-10) Performance Flight Research: Flight Data Report*. NASA/TM-20180000765.

<sup>4</sup>Jordan, T.; Langford, W.; Belcastro, C.; Foster, J.; Shah, G.; Howland, G.; Kidd, R.: *Development of a Dynamically Scaled Generic Transport Model Testbed for Flight Research Experiments*. NASA/TM-20040085988